DMD Fast Forward. Published on May 22, 2014 as doi:10.1124/dmd.114.057976

Evaluation of organic anion transporting polypeptide 1B1 and 1B3 humanized mice as a translational model to study the pharmacokinetics of statins

Laurent Salphati, Xiaoyan Chu, Liangfu Chen, Bhagwat Prasad, Shannon Dallas, Raymond Evers, Donna Mamaril-Fishman, Ethan G. Geier, Jonathan Kehler, Jeevan Kunta, Mario Mezler, Loic Laplanche, Jodie Pang, Anja Rode, Matthew G. Soars, Jashvant D. Unadkat, Robert A.B. van Waterschoot, Jocelyn Yabut, Alfred H. Schinkel and Nico Scheer

DMPK and Bioanalytical Research, Abbvie Deutschland GmbH & Co. KG, Ludwigshafen, Germany (MM, LL, RvW). Current affiliation of RvW: Roche Pharma Research and Early Development (pRED), Department of Pharmaceutical Sciences, F. Hoffmann-La Roche Ltd. Basel, Switzerland

Metabolism and Pharmacokinetics, Bristol-Myers Squibb, Wallingford, Connecticut, USA (MGS)

Genentech, Inc., 1 DNA Way, South San Francisco, CA 94080, USA (LS, JP, EGG)

Drug Metabolism and Pharmacokinetics, GlaxoSmithKline Pharmaceuticals, King of Prussia, Pennsylvania, USA (LC, DMF, JKe)

Janssen Research and Development, LLC, Spring House, PA, USA (SD, JKu).

Merck Sharp & Dohme Corporation, Whitehouse Station, New Jersey, USA (XC, JY, and RE)

Department of Pharmaceutics, University of Washington, Seattle, P.O. Box 357610, WA 98195, USA (BP, JDU)

Division of Molecular Oncology, The Netherlands Cancer Institute, Amsterdam, The Netherlands (AHS)

TaconicArtemis, Neurather Ring 1, Koeln 51063, Germany (AR, NS).

DMD Fast Forward. Published on May 22, 2014 as DOI: 10.1124/dmd.114.057976
This article has not been copyedited and formatted. The final version may differ from this version.

Running title: OATP1B1 and -1B3 humanized mice

Address correspondence to:

Nico Scheer, PhD, TaconicArtemis, Neurather Ring 1, 51063 Koeln, Germany.

Tel.: +49 221 9645343; Fax: +49 221 9645321; Email: nico.scheer@taconicartemis.com

Number of text pages: 26

Number of Tables: 3

Number of Figures: 7

Number of references: 38

Number of words in Abstract: 237

Number of words in Introduction: 743

Number of words in Discussion: 1878

Nonstandard abbreviations used:

Ces, carboxylesterase; DDIs, drug-drug interactions; hOATP1B1, OATP1B1 humanized mice; hOATP1B3, OATP1B3 humanized mice; hOATP1B1/1B3, OATP1B1 and -1B3 double humanized mice; OATP, organic anion transporting polypeptide; Oatp1a/1b KO, *Slco1a*/*1b* gene cluster knockout mice; qRT-PCR; quantitative real time PCR; WT, wild type

DMD Fast Forward. Published on May 22, 2014 as DOI: 10.1124/dmd.114.057976
This article has not been copyedited and formatted. The final version may differ from this version.

Abstract

Organic anion transporting polypeptide (Oatp) 1a/1b knockout and OATP1B1 and -1B3 humanized mouse models are promising tools for studying the roles of these transporters in drug disposition. Detailed characterization of these models will help to better understand their utility for predicting clinical outcomes. In order to advance this approach, we carried out a comprehensive analysis of these mouse lines by evaluating the compensatory changes in mRNA expression, quantifying the amounts of OATP1B1 and -1B3 protein by LC-MS/MS, studying the active uptake in isolated hepatocytes and the pharmacokinetics of some prototypical substrates including statins. Major outcomes from these studies were (1) mostly moderate compensatory changes in only a few genes involved in drug metabolism and disposition, (2) a robust hepatic expression of OATP1B1 and -1B3 proteins in the respective humanized mouse models, and (3) functional activities of the human transporters in hepatocytes isolated from the humanized models with several substrates tested in vitro and with pravastatin in vivo. However, the expression of OATP1B1 and -1B3 in the humanized models did not significantly alter liver or plasma concentrations of rosuvastatin and pitavastatin compared to Oatp1a/1b knockout controls under the conditions employed in our studies. Hence, while the humanized OATP1B1 and -1B3 mice showed in vitro and /or in vivo functional activity with some statins, further characterization of these models is required to define their potential use and limitations in the prediction of drug disposition and drug-drug interactions in human.

DMD Fast Forward. Published on May 22, 2014 as DOI: 10.1124/dmd.114.057976
This article has not been copyedited and formatted. The final version may differ from this version.

Introduction

The human organic anion transporting polypeptides (OATP) 1B1 and 1B3 are members of the OATP class of proteins, which are encoded by the *SLCO* gene family (Hagenbuch and Meier, 2004). Both OATP1B1 and -1B3 are expressed in the liver and are increasingly recognized as important hepatic uptake transporters for many classes of drugs, such as 3-hydroxyl-3-methylglutaryl-CoA reductase inhibitors (statins), angiotensin II receptor antagonists (sartans), and several anticancer drugs (Ieiri et al., 2009). As a consequence, inhibition of OATP1B transporters may cause clinically significant drug-drug interactions (DDIs) (Kalliokoski and Niemi, 2009; Yoshida et al., 2012; Shitara et al., 2013) and genetic polymorphisms of these transporters can result in significant inter-individual differences in the pharmacokinetics and pharmacodynamics of such compounds (Ieiri et al., 2009; Niemi et al., 2011), which sometimes can lead to severe toxicity (Morimoto et al., 2004; Konig et al., 2006; Link et al., 2008; Takane et al., 2009). For example, common variants in *SLCO1B1* were found to be strongly associated with an increased risk of statin-induced myopathy in a genome-wide association study (Link et al., 2008). Accordingly, the assessment of the potential for DDIs of new chemical entities (NMEs) with OATP1B1 and -1B3 has been recommended during drug development (Giacomini et al., 2010; European Medicine Agency (EMA), 2012; U.S. Department of Health and Human Services, 2012.).

The extrapolation of in vitro results to in vivo in humans is challenging and the predictability of traditional preclinical animal models is limited by the significant species differences in the level of sequence identity, expression pattern and substrate specificity of OATP1B proteins (Hagenbuch and Meier, 2003; Chu et al., 2013a; Grime and Paine, 2013). In addition, human livers express OATP1B1, 1B3 and 2B1, while mouse livers contain Oatp1a1, 1a4, 1b2 and 2b1. In an attempt to overcome these limitations, humanized mouse models for OATP1B1 or -1B3 have been generated (van de Steeg et al., 2012) by crossing OATP1B1 and -1B3

DMD Fast Forward. Published on May 22, 2014 as DOI: 10.1124/dmd.114.057976
This article has not been copyedited and formatted. The final version may differ from this version.

transgenic mice to a mouse model lacking all mouse *Slco1a* and *-1b* genes (Oatp1a/1b KO) (van de Steeg et al., 2012). In these models the human transporters are expressed under the control of the liver-specific apoE-promoter and it was estimated by Western blot analysis that the hepatic expression levels of the transgenic proteins were similar to those seen in pooled human liver samples. However, the protein levels were not determined quantitatively. Furthermore, the expression of both human transporters reversed the significant increase in plasma and urine levels of bilirubin monoglucuronide and bilirubin diglucuronide observed in Oatp1a/1b KO mice (van de Steeg et al., 2012). These results demonstrated (1) the in vivo role of human OATP1B1 and -1B3 in bilirubin glucuronide uptake and (2) the functional activity of the transgenic transporters in the humanized models. Similarly, subsequent studies in the humanized models showed partial reversal of the changes in liver and/or plasma levels observed in Oatp1a/1b KO animals (vs. wild type (WT) controls) with the anticancer drug methotrexate (van de Steeg et al., 2013) and the glucuronic acid metabolite of sorafenib (Zimmerman et al., 2013). Transgenic OATP1B3, but not OATP1B1, also was found to correlate with transport of paclitaxel in vivo (van de Steeg et al., 2013). Furthermore, three different statins (pravastatin, atorvastatin and simvastatin) and carboxydichlorofluorescein were very recently tested in Oatp1a/1b KO, hOATP1B1 and hOATP1B3 mice and it was concluded that systemic exposure and liver distribution changes in the humanized versus knockout mice may be used to predict the impact of the human transporters on clinical pharmacokinetics if the differences in protein expression of OATP1B1 and -1B3 in the humanized mice versus human liver are taken into account (Higgins et al., 2013).

Despite these reports, a more comprehensive characterization of the humanized models and understanding of the pharmacokinetics of different OATP1B substrates in these mice are needed before they can be used for mechanistic understanding and translational studies in drug development. To this end, we investigated potential compensatory gene expression

changes in the humanized OATP1B1 and -1B3 mice by mRNA analysis, quantified the protein amount of OATP1B1 and -1B3 in the liver of the humanized mice and compared those with human livers, tested various OATP1B substrates in isolated hepatocytes and conducted pharmacokinetic studies of three hydrophilic statins: pravastatin, rosuvastatin and pitavastatin, which are recommended OATP1B probe substrates for clinical DDI studies (U.S. Department of Health and Human Services, 2012.). Furthermore, we generated an OATP1B1/1B3 double humanized mouse model (hOATP1B1/1B3) to allow the assessment of the combined role of both transporters in the disposition of substrates in vivo, and we included these mice in some of our studies.

DMD Fast Forward. Published on May 22, 2014 as DOI: 10.1124/dmd.114.057976
This article has not been copyedited and formatted. The final version may differ from this version.

Materials and Methods

Chemicals and Reagents. Protein quantification: The ProteoExtract native membrane protein extraction kit was purchased from Calbiochem (Temecula, CA). The bicinchoninic acid (BCA) assay kit and the in-solution trypsin digestion kit were purchased from Pierce Biotechnology (Rockford, IL). Synthetic surrogate peptides and the corresponding stable isotope labeled (SIL) internal standards for human OATP1B1 and OATP1B3 were obtained from New England Peptides (Boston, MA) and Thermo Fisher Scientific (Rockford, IL), respectively. HPLC-grade acetonitrile and formic acid were purchased from Fischer Scientific (Fair Lawn, NJ) and Sigma-Aldrich (St. Louis, MO), respectively. In vitro studies: [^{3}H] Estradiol-17β-D-glucuronide ($E_2$17βG) (34.3 Ci/mmol), [^{3}H] cholecystokinin octapeptide (CCK-8) (96 Ci/mmol), and [^{3}H] taurocholic acid (5 Ci/mmol) were purchased from PerkinElmer Life Sciences (Boston, MA). [^{3}H] Pitavastatin (5 Ci/mmol), [^{3}H] rosuvastatin (10 Ci/mmol), [^{3}H] pravastatin (5 Ci/mmol), [^{3}H] atorvastatin (10 Ci/mmol), and [^{14}C] tetraethylammonium (TEA) (0.055 Ci/mmol), as well as unlabeled pitavastatin, rosuvastatin, pravastatin, and atorvastatin were purchased from American Radiolabeled Chemicals (St. Louis, MO). Rifamycin SV (RIF SV), rifampin and cyclosporin A (CsA) were purchased from Sigma-Aldrich (St. Louis, MO). Bromosulfophthalein (BSP) was purchased from MP Biomedicals (Solon, OH). In vivo studies: Pravastatin sodium, rosuvastatin and pitavastatin were purchased from Toronto Research Chemicals (Toronto, Canada), Sequoia Research Products (Berkshire, UK) and Allichem LLC (Baltimore, MD), respectively. All other reagents were commercially obtained with the highest analytical purity grade.

Mouse models, husbandry and experimentation. Oatp1a/1b KO, hOATP1B1 and hOATP1B3 mice were described previously (van de Steeg et al., 2010; van de Steeg et al., 2012; van de Steeg et al., 2013). Double humanized hOATP1B1/1B3 mice on a mouse

DMD Fast Forward. Published on May 22, 2014 as DOI: 10.1124/dmd.114.057976
This article has not been copyedited and formatted. The final version may differ from this version.

Slco1a/1b gene cluster knockout background were generated from hOATP1B1 and hOATP1B3 mice by breeding. Homozygous males from each strain and age-matched wild type (WT) controls, all on FVB genetic background, were obtained from Taconic Farms, Inc (Hudson, NY). Animals were allowed to acclimatize for at least five days prior to an experimental procedure at all experimental locations. Mice were kept in accord with local laws and regulations and in temperature-controlled environments with a 12-hour light cycle and given standard diets and water ad libitum. All animal procedures were approved by the local Institutional Animal Care and Use Committees.

mRNA measurements. (a) qRT-PCR: RNA extraction and reverse transcriptase PCR. Total RNA was extracted from the livers of WT, Oatp1a/1b KO, hOATP1B1, and hOATP1B3 mice (n=3/genotype) with the RNeasy Mini Kit (Qiagen, Valencia, CA), according to the kit instructions, and stored at -80°C after isolation. Total RNA (up to 1 μg) was reverse transcribed using the SuperScript VILO cDNA Synthesis Kit (Life Technologies, Carlsbad, CA) according to the manufacturer's instructions. The resulting cDNA samples were stored at -80°C.

Real time-PCR (RT-PCR) reactions were carried out in 96-well reaction plates in a volume of 10 μL using the TaqMan Fast Universal Master Mix, 5 ng of template cDNA, and TaqMan probes (Life Technologies) for mouse and human genes listed in Fig. 1. Reactions were run in duplicate for each gene per sample on an Applied Biosystems 7500 Fast Real-Time PCR System with the following profile: 95°C for 20 seconds followed by 40 cycles of 95°C for 3 seconds and 60°C for 30 seconds. The relative expression of each gene was calculated based on the $\Delta\Delta C_T$ comparative expression method (Pfaffl, 2001). The ΔC_T values for all the genes in each sample were calculated by subtracting the mean C_T values for two housekeeping genes (Gapdh and β-Actin) from the C_T for each target gene. The relative quantity of each gene was then determined by calculating $2^{-\Delta C_T}$.

DMD Fast Forward. Published on May 22, 2014 as DOI: 10.1124/dmd.114.057976
This article has not been copyedited and formatted. The final version may differ from this version.

(b) Microarray analysis: Animals were euthanized via CO_2 asphyxiation and a midline incision was made. The median lobe of the liver was removed and ~400 mg tissue pieces were snap frozen in liquid nitrogen. Following weighing, the frozen tissue was homogenized in Buffer RLT from a Qiagen Miniprep kit (Qiagen, Alameda, CA). Homogenized lysate was transferred to a clean conical tube and centrifuged at 5100 rpm for 10 min. 70% ethanol was added to the recovered supernatant, and centrifuged for 5 minutes in a spin column. RNA on the column filter was washed and recovered from the filter. Samples were stored at -80^{o}C until reverse transcription. 50 ng of total RNA was reverse transcribed and amplified using the Ovation RNA Amplification System V2 (NuGEN, San Carlos CA). cDNA was purified using Agencourt magnetic beads (Beckman Coulter, Brea CA) and normalized to 17 ng/ul on a Caliper SciClone ALH3000 robotic workstation (Perkin Elmer, Waltham MA). cDNA was then fragmented and labelled for hybridization using the Encore Biotin Module (NuGEN) according to the manufacturer's protocols. 1.875 µg of prepared target cDNA was hybridized to HT MG-430 PM arrays (Affymetrix, Santa Clara CA) for 16 hours at 48°C. Arrays were washed, stained and scanned using a GeneTitan instrument with MC Scanner (Affymetrix, Santa Clara, CA) according to manufacturer's protocols. Raw data for each sample was saved in standard CEL file format. The microarray raw data (CEL files) were processed and analysed using ArrayStudio version 6.0 software (Omicsoft, Cary, NC). Expression intensity of genes in each sample was extracted from CEL files using RMA algorithms and normalized across all samples using quantile normalization. Data quality was assessed by intensity distribution of each sample and Pearson correlation between samples in each genetic variation group. The average correlation in each group was 0.99 and all samples passed data quality assessment. Differential gene expression was identified by applying a general linear model that compares different genetic variations on normalized and log-2 transformed intensity data. Adjusted P value (Benjamini–Hochberg procedure) ($P<0.05$) and expression fold change (FC >2) were applied as cut-offs for selecting significant genes.

DMD Fast Forward. Published on May 22, 2014 as DOI: 10.1124/dmd.114.057976
This article has not been copyedited and formatted. The final version may differ from this version.

OATP1B1 and -1B3 protein quantification. Mice were euthanized at Taconic Farms, Inc. by exposure to a rising concentration of CO_2 and livers from 8-12 weeks old male Oatp1a/1b KO (n=2), hOATP1B1 (n=5) and hOATP1B3 (n=5) mice were extracted. The livers were cut into pieces of ~100 mg, rinsed several times with sterile PBS and flash frozen in liquid nitrogen and stored at -80°C until analysis. The liver tissue was processed as described before (Prasad et al., 2013) using the native membrane extraction kit (Calbiochem, Temecula, CA). Then, trypsin digestion was performed for 24 h with protein:trypsin ratio (25:1; w/w) after protein denaturation, reduction and alkylation following exactly the same protocol as described previously (Prasad et al., 2013). The reaction was quenched using 70% acetonitrile (containing SIL internal standard mix) and the samples were centrifuged at 4000 g for 5 min. Calibration standards were also prepared in the same manner except that the extraction buffer II of the kit was used instead of the membrane extracts. The synthetic surrogate peptides of human OATP1B1 (NVTGFFQSFK) and human OATP1B3 (NVTGFFQSLK) were used as the calibrators. The corresponding peptides containing labeled [13C615N2]-lysine residue were used as internal standards. Agilent 6460A triple-quadrupole mass spectrometer coupled to Agilent 1290 Infinity LC system (Agilent Technologies, Santa Clara, CA) operated using the optimized conditions (Prasad et al., 2013) was used for the transporter quantification.

In vitro studies. Isolation of primary mouse hepatocytes: Fresh primary mouse hepatocytes were isolated from male WT (FVB), Oatp1a/1b KO, hOATP1B1 and hOATP1B3 mouse livers (abbreviated as WT, Oatp1a/1b KO, hOATP1B1 and hOATP1B3 hepatocytes, respectively) using a two-step collagenase perfusion method (Li et al., 2010). Briefly, mice were anesthetized with 50 mg/mL nembutal. A catheter was placed into the inferior vena cava with flow (5ml/min) out through the portal vein. At 37°C, the first solution containing 0.5mM EGTA in Earle's basic salt solution without Ca^{2+}/Mg^{2+} was perfused to weaken the intercellular junctions of liver cells by removing extracellular calcium ions. The second

DMD Fast Forward. Published on May 22, 2014 as DOI: 10.1124/dmd.114.057976
This article has not been copyedited and formatted. The final version may differ from this version.

solution containing 300 μg/mL collagenase IV with Ca^{2+}/Mg^{2+} in Hanks basic salt solution was used to break down the extracellular compartment to easily release both non-parenchymal and parenchymal cell fractions. The isolated hepatocyte suspension was obtained after mechanical dissociation, filtration and low speed centrifugation. Following isolation of cells and 36% percoll purification, cell viability was measured (~70%) and hepatocytes were then prepared for uptake studies.

Uptake studies in hepatocytes: Uptake studies were conducted as described previously (Chu et al., 2013b) in fresh mouse hepatocyte suspensions. Briefly, cells were re-suspended in Krebs-Henseleit Modified Buffer (KHB) (Sigma-Aldrich, St. Louis, MO) (pH 7.4) in 96-deep well plates (Analytical Sales, Pompton Plains, NJ) at the final concentration of 0.2 x 10^6 cells/well. The cells and dosing solution were pre-incubated at 37°C for 5 min. Uptake studies were initiated by the addition of 50 μL radiolabeled substrate compounds. The reaction mixtures were incubated at 37°C for the time indicated and uptake was stopped by the addition of ice cold phosphate-buffered saline (PBS), followed by immediate centrifugation for 1 minute at 3000g at 4°C (Model 5180R; Eppendorf, Hamburg, Germany) and washing of the cell pellets with ice cold PBS for three times. Cell pellets were re-suspended in 50% acetonitrile, scintillation fluid (Scintisafe Econo 2; Fisher Chemicals, Pittsburgh, PA) was added, and radioactivity was determined by liquid scintillation counting in a LS6500 Multipurpose Scintillation Counter (Beckman Coulter). Inhibitory effect of several prototypical inhibitors of hepatic uptake transporters, including rifamycin SV, rifampin, cyclosporin A, BSP, and quinidine (Niemi et al., 2011), on uptake of test compounds was also measured at 3 min at 37°C.

In vivo studies. (a) Pravastatin. 9-14 weeks old mice from each of the different mouse lines and with numbers per dose group as described in the results section were used in the studies. Pravastatin was administered in saline either intravenously (IV) or orally (PO) at 5 mg/kg. A

DMD Fast Forward. Published on May 22, 2014 as DOI: 10.1124/dmd.114.057976
This article has not been copyedited and formatted. The final version may differ from this version.

crossover design was used in the pharmacokinetic studies; 4 mice from each strain were given an IV dose of 5 mg/kg pravastatin and 15 µL of blood was taken via tail nick at 0.033, 0.83, 0.25, 0.5, 1 and 2hrs post-dose. Blood was added to 60 µL of EDTA water then vortexed and stored at -80ºC until analysis. After a 7-day washout period, the same mice received a PO (5 mg/kg) dose of pravastatin. Following oral administration, blood was collected and processed as described for the IV administration. For liver concentration and liver-to-blood ratio determinations, 6 mice from each strain were given a PO dose (5 mg/kg). Animals were euthanized 5 or 30 minutes post-dose by terminal bleeding through cardiac puncture under isoflurane anesthesia and tissues were isolated. Liver was rinsed in phosphate buffered saline, weighed and stored at -80^{o}C until analysis. Approximately 200 µL of blood was collected into microtainer containing EDTA and centrifuged at 11,000 rpm for 5 minutes and plasma was collected and stored at -80^{o}C until analysis. 75 µL of blood was added to 300uL of EDTA water, votexed and stored at -80^{o}C until analysis.

(b) Rosuvastatin. Four animals per strain (WT, Oatp1a/1b KO, hOATP1B1 and hOATP1B3) were used for IV or PO administration of rosuvastatin. For IV bolus administration, the rosuvastatin dose was 5 mg/kg, in 2% N-methyl-*2*-pyrrolidone:10% Solutol, via tail vein. Following a two-week washout period, rosuvastatin was administered orally at 15 mg/kg in 0.5% hydroxypropyl methylcellulose to the same groups of mice through a gavage needle. Serial blood sampling procedures were followed as described by Peng et al. (2009). Plasma samples were collected at 2, 5, 15 and 30 min and 1, 2, 6 and 24 h following IV administration, and at 5, 15 and 30 min and 1, 2, 6 and 24 h after PO dosing (Peng et al., 2009).

(c). Pitavastatin. hOATP1B1, hOATP1B3, Oatp1a/1b KO and FVB/N WT mice (9, 9, 9, 12 animals) were dosed at 5 mg/kg PO. Blood samples were collected via composite sampling with three animals per group through microsampling from the saphenous vein at 6, 15, 30 min, and 1, 2, 3, 5 and 8 hours. At 15 min, 2 and 8 hours the groups of animal were deeply

DMD Fast Forward. Published on May 22, 2014 as DOI: 10.1124/dmd.114.057976
This article has not been copyedited and formatted. The final version may differ from this version.

anesthetized with isoflurane, euthanized; terminal bleeds taken from cardiac puncture, and liver was isolated and stored at -20°C until use. At each timepoint in both studies, blood samples were centrifuged at 4000 rpm for 10 min, plasma transferred to Micronic PP tubes, and stored at -20°C until use.

LC-MS/MS analysis. Details on the measurement of pravastatin, rosuvastatin, and pitavastatin blood, plasma, liver and /or urine concentration using liquid chromatography-tandem mass spectrometry (LC-MS/MS) are provided in the Supplementary Materials and Methods.

Pharmacokinetic analysis. Pharmacokinetic parameters were calculated by non-compartmental methods as described in Gibaldi and Perrier (Gibaldi and Perrier, 1982) using Phoenix™ WinNonlin® Version 6.3 or WinNonlin 5.2 (Pharsight Corporation, Mountain View, CA).

Statistical analysis. Student's t-test ($P<0.01$) or one-way ANOVA was applied to determine statistical significance in in vitro hepatocytes uptake studies (compared to Oatp1a/1b KO mice in uptake time course studies and corresponding no inhibitor control in inhibition studies). Pharmacokinetic parameters obtained with pravastatin and rosuvastatin were compared between the Oatp1a/1b KO mice and each of the other mouse strains by *t*-test and overall through one-way ANOVA. Values were considered statistically different when $p<0.05$. Analyses were done using Microsoft Excel or GraphPad Prism 5.

DMD Fast Forward. Published on May 22, 2014 as DOI: 10.1124/dmd.114.057976
This article has not been copyedited and formatted. The final version may differ from this version.

Results

Gene expression changes in Oatp1a/1b KO, hOATP1B1 and hOATP1B3 mice. To better understand potential compensatory changes in the expression of genes encoding proteins involved in drug metabolism and disposition, we compared hepatic mRNA levels of selected genes by quantitative real time PCR (qRT-PCR) as well as the whole genome by microarray analysis between wild type (WT), Oatp1a/1b KO, hOATP1B1 and hOATP1B3 mice.

(a) qRT-PCR: Liver expression of genes was determined by qRT-PCR for 17 transporters and 9 drug metabolizing enzymes selected for their involvement in drug transport or reported expression change in KO and humanized mice (van de Steeg et al., 2013). As expected, *Slco1a1*, *Slco1a4,* and *Slco1b2* were only detected in WT mice, while *SLCO1B1* and *SLCO1B3* were only detected in hOATP1B1 and hOATP1B3 mice, respectively (Fig. 1). This confirmed the successful deletion of mouse *Slco1a*/*1b* genes in the liver of Oatp1a/1b KO, hOATP1B1 and hOATP1B3 mice. Overall, few genes showed altered expression in the absence and/or presence of different Slco/SLCO transporters. Of the remaining 13 transporter genes, which were analysed, only *Abcb1b* showed an altered expression pattern, with mRNA expression increased by 4-6-fold in Oatp1a/1b KO and both strains of humanized mice relative to WT mice. Five metabolizing enzyme genes had altered expression patterns (> 2-fold change) across the different strains of mice (Fig. 1). *Aox1* (2-3-fold reduction), *carboxylesterase* (*Ces*) 1c (2-200-fold reduction), *Ces1d* (3-8-fold reduction), *Ces1e* (3-19-fold reduction), and *Ces2a* (2-fold reduction) all had reduced mRNA expression in Oatp1a/1b KO and both strains of humanized mice relative to WT mice. The strongest reduction in *Ces* gene expression was observed in hOATP1B1 followed by hOATP1B3 mice. Interestingly, Oatp1a/1b KO mice showed increased levels of hepatic *Ces1* expression in the study by (Iusuf et al., 2013a), which were normalized in hOATP1B1 and hOATP1B3 mice, while we found unchanged or slightly decreased *Ces1* levels in Oatp1a/1b KO mice in our analysis and a

DMD Fast Forward. Published on May 22, 2014 as DOI: 10.1124/dmd.114.057976
This article has not been copyedited and formatted. The final version may differ from this version.

more pronounced repression in the humanized mice (Fig. 1; Supplementary Table 1). This discrepancy might be explained by the different origins of the mouse lines (Netherlands Cancer Institute vs. Taconic Farms, Inc) and the possible impact of genetic drift or housing, and/or diet.

(b) Microarray analysis: Microarray analysis on mouse livers from WT, hOATP1B1, hOATP1B3 and Oatp1a/1b KO mice revealed a total of 294 unique genes (356 total genes, including genes that are duplicated within the array) altered by greater than 2-fold ($p < 0.05$). The full list of genes and the fold changes observed can be found in Supplementary Table 1. As expected, in Oatp1a/1b KO, hOATP1B1 and hOATP1B3 mice, the hepatic expression of the mouse *Slco1a1*, *Slco1a4* and *Slco1b2* genes was significantly suppressed compared to WT controls (43 to 239-fold decrease). No other significant changes in known "drug" transporter genes were noted with the exception of *Abcc9,* which compared to the WT mice was decreased by 2.3, 2.3 and 2.2-fold in Oatp1a/1b KO, hOATP1B1 and hOATP1B3 mice, respectively. Genes coding for members of the solute carrier superfamily of transporters that showed significant down-regulation included *Slc6a4* (serotonin transporter), *Slc13a2* (sodium/dicarboxylate co-transporter), *Slc26a3* (chloride anion exchanger), and *Slc30a10* (zinc transporter). Slc transporter genes that were significantly induced included *Slc5a3* (sodium/myo-inositol co-transporter), *Slc10a2* (sodium/bile acid co-transporter), *Slc25a32* (mitochondrial folate transporter) and *Slc43a1* (large neutral amino acid transporter).

In terms of genes encoding for drug metabolizing enzymes, in agreement with the qRT-PCR results, *Ces1d* and *1e* were significantly repressed, particularly when comparing hOATP1B1 to WT or Oatp1a/1b KO mice (23 to 364-fold repression, respectively). In general, *Ces1* gene expression in Oatp1a/1b KO mice was comparable to WT controls, while they were markedly repressed in the humanized models. The arylhydrocarbon receptor responsive cytochrome P450 (CYP) gene *Cyp2b9* showed greater than 4-fold repression in the knockout and

DMD Fast Forward. Published on May 22, 2014 as DOI: 10.1124/dmd.114.057976
This article has not been copyedited and formatted. The final version may differ from this version.

humanized mice, as compared to WT controls. The peroxisome proliferator-activated receptor alpha-responsive *Cyp4a10* and *Cyp4a14* genes were also repressed in the knockout and humanized mouse, when compared to WT mice. In contrast, two members of the flavin monoxygenase family (*Fmo2* and *3*), were upregulated > 2-fold in the humanized versus WT mice. Finally, Nicotinamide N-methyltransferase (*Nmnt*) was also induced in both the knockout and humanized mice, compared to WT controls (> 2.6- fold).

Quantification of hepatic OATP1B1 and -1B3 protein expression in hOATP1B1 and hOATP1B3 mice. The OATP1B1 and OATP1B3 protein amount in hOATP1B1 and hOATP1B3 mice was 1.63±0.08 and 3.83±1.31 fmol/µg of total membrane protein, respectively. The level of OATP1B3 in the liver of hOATP1B3 mice was on average 2.4-fold higher than the level of OATP1B1 in hOATP1B1 animals. The relative differences in hepatic OATP1B1 and -1B3 amounts between the hOATP1B1 and hOATP1B3 mice were similar as measured by three independent groups who contributed to this paper (data not shown). While the amount of hepatic OATP1B1 in hOATP1B1 mice (1.63±0.08 fmol/µg protein) was marginally lower than the previously determined average amount in human liver (2.0±0.9 fmol/µg protein) (Prasad et al., 2013), OATP1B3 was ~3.5 fold higher in hOATP1B3 mice than the average human levels (1.1 ± 0.5 fmol/µg protein) (Fig. 2). There was neither a signal for OATP1B1 peptide in hOATP1B3 mice or for OATP1B3 in hOATP1B1 mice, nor for any of the two human peptides in Oatp1a/1b KO animals. In the present study, to avoid variability in transporter quantification in human vs. animal tissues due to differences in laboratories or methods, the transporters were quantified by the same laboratory (and method) that quantified the transporters in the human liver tissues (Prasad et al., 2013).

Uptake studies in isolated hepatocytes. <u>(a) Uptake of prototypical substrates for hepatic uptake transporters into mouse hepatocytes:</u> Functional activity of uptake transporters in WT, Oatp1a/1b KO, hOATP1B1, and hOATP1B3 mouse livers was determined by measuring the

DMD Fast Forward. Published on May 22, 2014 as DOI: 10.1124/dmd.114.057976
This article has not been copyedited and formatted. The final version may differ from this version.

uptake of $E_2$17βG (0.1 μM), CCK-8 (0.01 μM), TEA (0.1 μM), and TCA (0.1 μM), prototypical substrates for OATP1B1, -1B3, OCT1, and NTCP, respectively (Brouwer et al., 2013), in hepatocytes freshly isolated from the above strains (Fig. 3). Uptake of $E_2$17βG was almost absent in hepatocytes from Oatp1a/1b KO mice, confirming that mouse Oatp1a/1b is responsible for hepatic uptake of this compound. In WT mouse hepatocytes uptake of $E_2$17βG was time-dependent and was abolished nearly completely in the presence of the OATP inhibitors RIF SV (100 μM), rifampin (200 μM), and CsA (10 μM). Uptake of $E_2$17βG in hOATP1B1 and hOATP1B3 hepatocytes was 3- to 10-fold higher than in Oatp1a/1b KO mice at all the time points tested, but 134- and 40-fold lower than in hepatocytes from WT mice (Fig. 3). As a selective probe substrate for OATP1B3, uptake of CCK-8 in hOATP1B3 mouse hepatocytes was time-dependent, and substantially higher than the uptake measured in hepatocytes from all other mouse strains (Fig. 3). The uptake of CCK8 in both hOATP1B3 and WT hepatocytes was completely inhibited by RIF SV (100 μM), rifampin (200 μM), and CsA (10 μM), indicating that OATP1B3 was functional in hOATP1B3 hepatocytes. Uptake of TEA, a prototypical substrate of OCT1/Oct1 was time-dependent and comparable in hepatocytes from all mouse strains tested, and significantly inhibited by quinidine, an inhibitor of OCT1. Similarly, TCA, a substrate for hepatic NTCP/Ntcp, showed comparable hepatic uptake in all mouse strains, although its uptake in WT mouse hepatocytes was slightly higher than in other strains at 3 and 5 min ($P<0.01$) (Fig. 3G). Uptake of TCA in all strains was completely inhibited by BSP (100 μM), an inhibitor of Ntcp. These data suggested that hepatocytes isolated from the various mouse strains retained comparable functional activity of Oct and Ntcp.

(b) Uptake of several clinically used OATP1B substrates into mouse hepatocytes: To further assess the functional activity of OATP1B1 and -1B3 in hOATP1B1 and hOATP1B3 mice, uptake of pitavastatin, rosuvastatin, pravastatin, and atorvastatin was evaluated in hepatocytes

DMD Fast Forward. Published on May 22, 2014 as DOI: 10.1124/dmd.114.057976
This article has not been copyedited and formatted. The final version may differ from this version.

isolated from all mouse strains. Compared to WT mice, uptake of all compounds tested was reduced substantially in Oatp1a/1b KO hepatocytes (Fig. 4), confirming that Oatp1a/1b is the predominant contributor to the hepatic uptake of these compounds in WT mouse hepatocytes. In hOATP1B1 hepatocytes, uptake of pitavastatin, rosuvastatin, and atorvastatin was higher than in Oatp1a/1b KO hepatocytes, but significantly lower than in WT hepatocytes. In the case of pravastatin, uptake in hOATP1B1 hepatocytes was only slightly higher than in Oatp1a/1b KO hepatocytes at 3 and 5 minutes ($P<0.01$) (Fig. 4E). Uptake measured in hOATP1B1 hepatocytes likely could be attributed to OATP1B1 as it was inhibited by RIF SV, rifampin, and CsA. Notably, the residual hepatic uptake of the statins (relatively high for pitavastain, atorvastatin, and rosuvastatin, but low for pravastatin) observed in Oatp1a/1b KO hepatocytes, was significantly inhibited by the above inhibitors. By contrast, uptake of statins in hOATP1B3 hepatocytes was compound dependent. Uptake of pravastatin and atorvastatin in hOATP1B3 hepatocytes was significantly higher than in hOATP1B1 hepatocytes, whereas uptake of other statins was within the same range as in hOATP1B1 hepatocytes. Hepatic uptake of all statins tested in hOATP1B3 hepatocytes was sensitive to RIF SV, rifampin, and CsA.

Pharmacokinetics of pravastatin, rosuvastatin and pitavastatin in WT, Oatp1a/1b KO, hOATP1B1 and hOATP1B3 mice. In vivo activities of OATP1B1 and -1B3 towards the OATP1B substrates pravastatin, pitavastatin, and rosuvastatin were assessed in pharmacokinetic studies in hOATP1B1 and -1B3 mice. In these studies, the effect of the transgenic transporters on systemic (plasma or blood) and liver exposure of the above statins was investigated.

(a) Pravastatin: In a first study pravastatin was tested in Oatp1a/1b KO, hOATP1B1, hOATP1B3 and WT mice. Following IV (5 mg/kg) administration of pravastatin, systemic exposure measured by blood AUC was 4-fold higher in Oatp1a/1b KO mice when compared

DMD Fast Forward. Published on May 22, 2014 as DOI: 10.1124/dmd.114.057976
This article has not been copyedited and formatted. The final version may differ from this version.

to WT animals (Fig. 5A, Table 1), with blood concentrations between these two strains significantly different at all time-points tested. Pravastatin blood concentrations in the hOATP1B1 and -1B3 mice were only slightly lower than those measured in Oatp1a/1b KO animals (Fig 5A), with AUC remaining 3.4- and 2.7-fold higher, respectively, than in the WT mice. In contrast, a more pronounced impact was observed following PO administration (Fig. 5B). Pravastatin AUC_{0-2} in Oatp1a/1b KO mice was 18-fold higher than in the WT animals, and exposure in the humanized mice pointed to a recovery of the liver uptake activity with systemic exposure in the hOATP1B1 and -1B3 mice 8.6- and 3.7-fold higher than in the WT, respectively, and significantly lower than that measured in the KO mice (Figure 5B, Study 1 in Table 1). Pravastatin liver concentrations measured 5 minutes following PO administration were ~2-fold lower in Oatp1a/1b KO than in the WT mice (data not shown). In hOATP1B1 animals, liver concentrations were 35% higher than in Oatp1a/1b KO mice, while in hOATP1B3 mice they were similar to Oatp1a/1b KO animals (data not shown). Liver concentrations were not significantly different between the four strains 30 minutes post-dose (data not shown). Changes in hepatic uptake were reflected more profoundly in the liver-to-blood ratio, which was significantly reduced in Oatp1a/1b KO mice (1.3 vs. 166 in WT mice). Although the ratio was only moderately restored in the humanized mice, it was significantly different from that measured in Oatp1a/1b KO animals 5 and 30 min post-dose (Fig. 5C; 2.1-4.4 in humanized mice vs. 1.3 in KO mice).

In a follow-up study, pravastatin was tested in Oatp1a/1b KO, hOATP1B1/1B3 and WT mice. The significant increase in systemic exposure in Oatp1a/1b KO mice compared to WT controls following IV administration was confirmed in this study. Interestingly, the pravastatin blood concentrations in hOATP1B1/1B3 mice were comparable to WT levels (Fig. 5D), in contrast to the minor reversion observed in the corresponding single humanized models (Fig. 5A). The pravastatin AUC_{0-2} in hOATP1B1/1B3 mice was also significantly

DMD Fast Forward. Published on May 22, 2014 as DOI: 10.1124/dmd.114.057976
This article has not been copyedited and formatted. The final version may differ from this version.

(3.7-fold) lower than in Oatp1a/1b KO mice after PO administration (Fig. 5E and Study 2 in Table 1), while sufficient data points above the limit of detection could not be collected in WT controls to establish a PK profile in this study. Nevertheless, measured blood concentrations at 0.25, 0.5, and 1 hrs were substantially lower than in both Oatp1a/1b KO, and hOATP1B1/1B3 mice.

(b) Pitavastatin: A 5 mg/kg PO dose of pitavastatin was administered to Oatp1a/1b KO, hOATP1B1, hOATP1B3 and WT mice. While pitavastatin plasma exposure in Oatp1a/1b KO mice was increased 11-fold compared to WT controls, the plasma concentration-time profile in hOATP1B1 and hOATP1B3 mice was not different from Oatp1a/1b KO animals (Fig. 6A, Table 2). Furthermore, the liver-to-plasma ratio was markedly decreased in Oatp1a/1b KO relative to WT animals (Fig. 6B), though the liver concentrations were not significantly different between the two mouse lines (data not shown). In contrast, pitavastatin liver concentrations in hOATP1B1 mice were numerically slightly (up to 2-fold) increased compared to Oatp1a/1b KO animals, contributing to an up to 2-fold higher liver-to-plasma ratio in hOATP1B1 compared to Oatp1a/1b KO mice at all three time points (Fig. 6B). While these results might suggest a role of OATP1B1 in liver uptake of this compound, they were not statistically significant ($p > 0.05$; Student t-test) at any of the three time points (Fig. 6B). The liver concentrations and liver-to-plasma ratio in hOATP1B3 mice were indistinguishable from that measured in Oatp1a/1b KO animals (Fig. 6B).

(c) Rosuvastatin: Oatp1a/1b KO mice showed higher systemic exposure than WT mice after both IV (5 mg/kg) and PO (15 mg/kg) administration of rosuvastatin, with 2.3 (IV)- and 45 (PO)-fold increased mean $AUC_{0\text{-last}}$ and 2.1 (IV)- and 33 (PO)-fold increased C_{max}, respectively (Table 3). Surprisingly, neither in the hOATP1B1 nor the hOATP1B3 mice was there a reversion towards WT levels; both humanized mouse lines showing similar systemic exposures as the Oatp1a/1b KO animals (Fig. 7; Table 3).

DMD Fast Forward. Published on May 22, 2014 as DOI: 10.1124/dmd.114.057976
This article has not been copyedited and formatted. The final version may differ from this version.

Discussion

In this paper, Oatp1a/1b KO, hOATP1B1 and hOATP1B3 mice have been characterized further to assess their potential use in translational research. For this purpose, compensatory gene expression changes were assessed, the amount of OATP1B1 and -1B3 with those in human livers were compared, and the functional activity of various OATP1B probe substrates were tested both in vitro and in vivo.

In general, no remarkable compensatory changes in the expression of drug transporter genes were observed in the transgenic mouse models compared to WT controls except for a moderate increase in the expression of *Abcb1b* (4-6-fold, qRT-PCR) (Fig. 1; Supplementary Table 1), which has a limited functional role in the liver. For drug metabolizing enzymes, the most notable change was the up to ~300-fold repression of genes encoding for the carboxylesterases Ces1c, 1d and 1e (Supplementary Table 1). Future studies will need to assess if the changes in mRNA levels do result in alterations at both protein and activity levels. Nevertheless, studies in the transgenic mice should be undertaken cautiously for compounds containing an ester functional group, since the changes in the expression of carboxylesterases can be a confounding factor, as was recently described for the Ces-dependent conversion of irinotecan to its active and toxic metabolite SN-38 (Iusuf et al., 2013a).

When translating the data from humanized OATP1B mice to the human situation, it is important to compare the amount of hepatic OATP1B protein in the humanized mice relative to human liver. Using LC-MS/MS-based protein quantification we found that the amount of OATP1B3 in hOATP1B3 mice was 3.5-fold higher than the average level in human liver, while the expression of OATP1B1 in hOATP1B1 mice was comparable to that in human liver (Prasad et al., 2013). These results are in reasonable agreement with those recently reported

DMD Fast Forward. Published on May 22, 2014 as DOI: 10.1124/dmd.114.057976
This article has not been copyedited and formatted. The final version may differ from this version.

by Higgins et al (Higgins et al., 2013). Overall, these findings suggested that the effect of hOATP1B3 could be overestimated in this mouse model. It should be noted that the amount of OATP1B1 and -1B3 in this study was determined using crude membrane preparations from liver samples, without considering the specific spatial expression of the functional OATP1B in the plasma membrane within the liver.

Given that the in vivo disposition of many OATP1B substrates, such as statins, is complex, involving multiple elimination pathways via various drug transporters and metabolizing enzymes (Elsby et al., 2012; Yoshida et al., 2012), we evaluated the functional activity of hOATP1B mice using several OATP1B substrates both in isolated hepatocytes and in vivo. Using this comprehensive approach, we could directly measure the functional activity of OATP1B as active uptake transporters in vitro and assess their roles on in vivo disposition. For most of the compounds tested the expected increase in uptake in hepatocytes from the hOATP1B1 and hOATP1B3 mice relative to the Oatp1a/1b KO hepatocytes was observed, albeit in most cases not with a full recovery to WT levels (with the exception of CCK-8 in hOATP1B3 hepatocytes) (Figs. 3 and 4). The lack of full recovery was not unexpected, because five functional mouse Oatp1a/1b proteins were replaced with only one functional OATP1B transporter, OATP1B1 or -1B3, in the humanized mice. At the concentrations tested (0.1μM, typically at least 10-fold lower than reported K_m values of these OATP substrates) (Hirano et al., 2006; Kalliokoski and Niemi, 2009), a very obvious trend was the consistently lower uptake in hOATP1B1 compared to hOATP1B3 hepatocytes, except for pitavastatin and rosuvastatin, for which it was similar (Fig, 4). This trend may be explained by the 2.4-fold higher expression level of OATP1B3 in liver of the hOATP1B3 mice compared to OATP1B1 in hOATP1B1 animals. Surprisingly, a very weak recovery of pravastatin uptake in hOATP1B1 relative to Oatp1a/1b KO hepatocytes was observed, which contrasts with the in vivo results (see below).

DMD Fast Forward. Published on May 22, 2014 as DOI: 10.1124/dmd.114.057976
This article has not been copyedited and formatted. The final version may differ from this version.

To assess in vivo functional roles of OATP1B in hOATP1B mice, pharmacokinetic studies were conducted with pravastatin, pitavastatin, and rosuvastatin. In contrast to minimal in vitro functional activity of OATP1B1, a 2-fold decrease of pravastatin blood AUC in hOATP1B1 relative to Oatp1a/1b KO mice following PO dosing was observed. Despite the minimal changes measured after IV dosing of pravastatin, results obtained following PO administration (AUC and liver-to-blood ratios) suggested that OATP1B1 was functionally active in vivo in the hOATP1B1 mice. Nevertheless, our study design did not allow us to estimate hepatic CL and thus confirm unequivocally that the lower systemic exposure resulted from OATP1B1-mediated hepatic uptake. The mechanism explaining the lack of in vitro to in vivo translation is currently not known. Kinetic studies with pravastatin in hOATP1B1 hepatocytes could potentially help to explain such discrepancies. In contrast, hOATP1B3 demonstrated a more profound functional effect with significantly lower systemic AUC relative to Oatp1a/1b KO mice following both IV and PO dosing (1.5- and 4.7-fold, respectively). This is in agreement with the 5-fold higher uptake rate in hOATP1B3 mouse hepatocytes relative to hOATP1B1 and Oatp1a/1b KO mice. The functional activity of OATP1B1 and -1B3 in the humanized mice was further substantiated by the significant decrease of both IV and PO exposure of pravastatin in hOATP1B1/1B3 relative to Oatp1a/b KO mice (Fig. 5D, E; Table 1), in which case the IV exposure indeed decreased to almost WT levels. Interestingly, in a recent report by Higgins et al. (Higgins et al., 2013), hOATP1B1 mice only showed very modest in vivo functional activity following oral administration of pravastatin, compared to IV dosing. In contrast, a much stronger effect was observed in this study after PO administration (Fig. 5A, B). These differences might be explained by the markedly different doses used by Higgins et al. (10 mg/kg IV and 100 mg/kg PO, in which hepatic uptake transporters are likely saturated following oral administration) than in our studies (5 mg/kg for both IV and PO).

One of the unexpected findings was the lack of differences in systemic exposure for

DMD Fast Forward. Published on May 22, 2014 as DOI: 10.1124/dmd.114.057976
This article has not been copyedited and formatted. The final version may differ from this version.

pitavastatin and rosuvastatin in the hOATP1B1 and -1B3 mice compared to Oatp1a/1b KO animals. This was surprising, because of the established role of specifically OATP1B1 in the transport of these compounds in humans (Ieiri et al., 2009; Niemi et al., 2011; Williamson et al., 2013; Prueksaritanont et al., 2014) and the fact that the uptake of both compounds in hepatocytes derived from hOATP1B1 and hOATP1B3 mice was increased relative to Oatp1a/1b KO hepatocytes (Fig. 4). Lack of OATP1B1 functional activity with pitavastatin and rosuvastatin in vivo might be related to (1) potentially low transport activity in the liver of the hOATP1B1 mice. This is supported by less than 2-fold difference of uptake rate for both pitavastatin and rosuvastatin in hOATP1B1 relative to Oatp1a/1b KO hepatocytes (Fig. 3). Consistently, lower in vitro transport activity of OATP1B1 relative to OATP1B3 was also observed with several other OATP1B prototypical substrates tested (Figs 3 and 4). (2) Potential predominant effects of some other mouse transporters on hepatic uptake at in vivo relevant exposure. The residual hepatic uptake of pitavastain and rosuvastatin observed in Oatp1a/1b KO hepatocytes, was significantly inhibited by RIF SV, rifampicin and CsA (Fig. 4B, D), suggesting the differential involvement of other transporters in the hepatic uptake of these compounds (Ho et al., 2006; Bi et al., 2013). Relatively low impact and selectivity of OATP1B1 on overall in vivo disposition of rosuvastatin in humans may also explain minimal restoration of its systemic exposure in hOATP1B1 mice (Elsby et al., 2012; Prueksaritanont et al., 2014). (3) Potential change of alternative elimination pathways in hOATP1B mice. According to Insuf et al. renal clearance of rosuvastatin is only 9.4% of total clearance in WT mice (Iusuf et al., 2013b). However, renal clearance increased to 29% of total clearance in Oatp1a/1b KO mice, which is similar to humans. In fact, we observed increased renal excretion of rosuvastatin in humanized OATP1B1 and -1B3 and Oatp1a/1b KO mice relative to WT animals (preliminary observations, data not shown). This change in renal clearance may still not be the major explanation for the lack of in vivo functional activity of OATPs with rosuvastatin in the humanized mice. (4) Differences in the metabolism of these statins in

DMD Fast Forward. Published on May 22, 2014 as DOI: 10.1124/dmd.114.057976
This article has not been copyedited and formatted. The final version may differ from this version.

mice and humans, which might obscure the in vivo impact of the OATP1B transporters on drug disposition in the mouse models. The metabolism of rosuvastatin in mice was very limited (Hirano et al., 2005; Kitamura et al., 2008; Iusuf et al., 2013b), so that this appears to be an unlikely explanation for rosuvastatin. However, pitavastatin showed more profound hepatic metabolism in mice compared to rat and humans (Fujino et al., 2002). Despite more extensive metabolism, we observed ~12-fold increase of pitavastatin plasma AUC in Oatp1a/1b KO vs. WT mice, suggesting that Oatp1a/1b proteins play important roles in hepatic uptake of pitavastatin in mice. We cannot exclude however that the metabolism of pitavastatin in mice could be another contributing factor to the lack of difference in plasma exposure of pitavastatin between hOATP1B1 and Oatp1a/1b KO mice. Given that we did not observe significant compensatory changes of major drug metabolizing enzymes in these mouse strains, the changes of metabolic activity of pitavastatin in these mouse strains is less likely. Nevertheless, the detailed comparison of metabolic clearance of pitavastatin between these animals and humans could be helpful to understand the mechanism underlying the lack of in vivo functional activity of OATP1B1 with pitavastatin in the humanized mice.

Although the in vivo functionality of OATP1B with several substrates has been demonstrated in the humanized OATP1B mouse models (Higgins et al., 2013; van de Steeg et al., 2013; Zimmerman et al., 2013), quantitative translation of these findings to humans is still premature. In this study, only pravastatin showed in vivo functional activity of OATP1B1 and -1B3. Using the approach proposed by Higgins et al (Higgins et al., 2013), the fractional contribution of OATP1B1 to oral systemic clearance was estimated to be 0.57 (OATP1B1 relative expression factor is 1.23, Oatp1a/1b KO AUC_{po}/OATP1B1 AUC_{po} is 2.08), resulting in the maximal fold increase in systemic exposure of 2.3-fold. This is in agreement with the result by Higgins et al. However, when taking into account OATP1B3, the fractional contribution of OATP1B3 to oral systemic clearance was 0.52 (OATP1B3 relative expression factor is 0.29, Oatp1a/1b KO AUC_{po}/OATP1B3 AUC_{po} is 4.76), resulting in a maximal fold

increase in systemic exposure of 2.1-fold. As such, the impact of OATP1B3 was overestimated compared to clinical observations (Ieiri et al., 2009; Elsby et al., 2012). The lack of in vivo function with pitavastatin and rosuvastatin in hOATP1B1 mice might suggest that the activity is compound-dependent and preclude the translation of the findings for these two statins from humanized mice to humans. Furthermore, appropriate in vivo study design (e.g., IV and PO, and dose level) is critical to ensure relevant in vivo exposure is achieved compared to clinical studies. Finally, in vitro uptake studies in hepatocytes isolated from these mouse strains could be a useful tool to directly assess active hepatic uptake of OATP1B in these models. Detailed kinetic studies in the hepatocytes will be helpful to translate the in vitro observations to the in vivo situation, when taking into account relevant in vivo exposure, the ADME properties of drugs, and involvement of other transporters to their liver uptake. Further studies will be undertaken by our group to refine the mechanistic understanding of the observations reported here and to provide additional insights into the potential use of these models in translational research.

DMD Fast Forward. Published on May 22, 2014 as DOI: 10.1124/dmd.114.057976
This article has not been copyedited and formatted. The final version may differ from this version.

Acknowledgements

We wish to thank Aysel Güler, Ina Mairhofer and Dan Bow (Abbvie); Xiaolin Zhang (Genentech); Matthew Szapacs, Caroline Sychterz, Tanya Aldinger, Jessica Gannon Esaie Pierre, Debra Paul, Mike Hobbs (GSK); Monica Singer, Anton Bittner, Xiang Yao (Janssen); Aihua Zhang, Robert Houle, Sandra Tetteh, Xiaoxin Cai, Meihong Lin, and Grace Chan (MSD) for technical assistance.

DMD Fast Forward. Published on May 22, 2014 as DOI: 10.1124/dmd.114.057976
This article has not been copyedited and formatted. The final version may differ from this version.

Authorship Contributions

Participated in research design: LS, XC, LC, BP, SD, RE, EGG, JKu, LL, JDU, RvW, AHS, NS

Conducted experiments: LS, XC, LC, BP, DMF, EGG, JKe, JP, AR, RvW, JY

Performed data analysis: LS, XC, LC, BP, SD, RE, EGG, JKu, JP, MM, MGS, JDU, RvW, AHS, NS

Wrote or contributed to the writing of the manuscript: LS, XC, LC, BP, SD, RE, EGG, JKu, MM, MGS, JDU, RvW, AHS, NS

References

Bi YA, Qiu X, Rotter CJ, Kimoto E, Piotrowski M, Varma MV, Ei-Kattan AF and Lai Y (2013) Quantitative assessment of the contribution of sodium-dependent taurocholate co-transporting polypeptide (NTCP) to the hepatic uptake of rosuvastatin, pitavastatin and fluvastatin. *Biopharm Drug Dispos* **34:**452-461.

Brouwer KL, Keppler D, Hoffmaster KA, Bow DA, Cheng Y, Lai Y, Palm JE, Stieger B and Evers R (2013) In vitro methods to support transporter evaluation in drug discovery and development. *Clin Pharmacol Ther* **94:**95-112.

Chu X, Bleasby K and Evers R (2013a) Species differences in drug transporters and implications for translating preclinical findings to humans. *Expert Opin Drug Metab Toxicol* **9:**237-252.

Chu X, Cai X, Cui D, Tang C, Ghosal A, Chan G, Green MD, Kuo Y, Liang Y, Maciolek CM, Palamanda J, Evers R and Prueksaritanont T (2013b) In vitro assessment of drug-drug interaction potential of boceprevir associated with drug metabolizing enzymes and transporters. *Drug Metab Dispos* **41:**668-681.

Elsby R, Hilgendorf C and Fenner K (2012) Understanding the critical disposition pathways of statins to assess drug-drug interaction risk during drug development: it's not just about OATP1B1. *Clin Pharmacol Ther* **92:**584-598.

European Medicine Agency (EMA) CfHMPC (2012) Guideline on the investigation of drug interactions. 21 June 2012.

Fujino H, Yamada I, Shimada S and Kojima J (2002) Metabolic fate of pitavastatin, a new inhibitor of HMG-CoA reductase--effect of cMOAT deficiency on hepatobiliary excretion in rats and of mdr1a/b gene disruption on tissue distribution in mice. *Drug Metab Pharmacokinet* **17:**449-456.

Giacomini KM, Huang SM, Tweedie DJ, Benet LZ, Brouwer KL, Chu X, Dahlin A, Evers R, Fischer V, Hillgren KM, Hoffmaster KA, Ishikawa T, Keppler D, Kim RB, Lee CA, Niemi M, Polli JW, Sugiyama Y, Swaan PW, Ware JA, Wright SH, Yee SW, Zamek-Gliszczynski MJ and Zhang L (2010) Membrane transporters in drug development. *Nat Rev Drug Discov* **9:**215-236.

Gibaldi M and Perrier D (1982), in: *Pharmacokinetics*, pp 332-333, Marcel Dekker, Inc., NewYork/Basel.

Grime K and Paine SW (2013) Species differences in biliary clearance and possible relevance of hepatic uptake and efflux transporters involvement. *Drug Metab Dispos* **41:**372-378.

Hagenbuch B and Meier PJ (2003) The superfamily of organic anion transporting polypeptides. *Biochim Biophys Acta* **1609:**1-18.

Hagenbuch B and Meier PJ (2004) Organic anion transporting polypeptides of the OATP/ SLC21 family: phylogenetic classification as OATP/ SLCO superfamily, new nomenclature and molecular/functional properties. *Pflugers Arch* **447:**653-665.

Higgins JW, Bao JQ, Ke AB, Manro JR, Fallon JK, Smith PC and Zamek-Gliszczynski MJ (2013) Utility of oatp1a/1b-knockout and OATP1B1/3-humanized Mice in the Study of OATP-mediated Pharmacokinetics and Tissue Distribution: Case Studies with Pravastatin, Atorvastatin, Simvastatin, and Carboxydichlorofluorescein. *Drug Metab Dispos*.

Hirano M, Maeda K, Matsushima S, Nozaki Y, Kusuhara H and Sugiyama Y (2005) Involvement of BCRP (ABCG2) in the biliary excretion of pitavastatin. *Mol Pharmacol* **68:**800-807.

Hirano M, Maeda K, Shitara Y and Sugiyama Y (2006) Drug-drug interaction between pitavastatin and various drugs via OATP1B1. *Drug Metab Dispos* **34:**1229-1236.

Ho RH, Tirona RG, Leake BF, Glaeser H, Lee W, Lemke CJ, Wang Y and Kim RB (2006) Drug and bile acid transporters in rosuvastatin hepatic uptake: function, expression, and pharmacogenetics. *Gastroenterology* **130:**1793-1806.

Ieiri I, Higuchi S and Sugiyama Y (2009) Genetic polymorphisms of uptake (OATP1B1, 1B3) and efflux (MRP2, BCRP) transporters: implications for inter-individual differences in the pharmacokinetics and pharmacodynamics of statins and other clinically relevant drugs. *Expert Opin Drug Metab Toxicol* **5:**703-729.

Iusuf D, Ludwig M, Elbatsh A, van Esch A, van de Steeg E, Wagenaar E, van der Valk M, Lin F, van Tellingen O and Schinkel AH (2013a) OATP1A/1B transporters affect irinotecan and SN-38 pharmacokinetics and carboxylesterase expression in knockout and humanized transgenic mice. *Mol Cancer Ther*.

Iusuf D, van Esch A, Hobbs M, Taylor M, Kenworthy KE, van de Steeg E, Wagenaar E and Schinkel AH (2013b) Murine Oatp1a/1b uptake transporters control rosuvastatin systemic exposure without affecting its apparent liver exposure. *Mol Pharmacol* **83:**919-929.

Kalliokoski A and Niemi M (2009) Impact of OATP transporters on pharmacokinetics. *Br J Pharmacol* **158:**693-705.

Kitamura S, Maeda K, Wang Y and Sugiyama Y (2008) Involvement of multiple transporters in the hepatobiliary transport of rosuvastatin. *Drug Metab Dispos* **36:**2014-2023.

Konig J, Seithel A, Gradhand U and Fromm MF (2006) Pharmacogenomics of human OATP transporters. *Naunyn Schmiedebergs Arch Pharmacol* **372:**432-443.

Li WC, Ralphs KL and Tosh D (2010) Isolation and culture of adult mouse hepatocytes. *Methods Mol Biol* **633:**185-196.

Link E, Parish S, Armitage J, Bowman L, Heath S, Matsuda F, Gut I, Lathrop M and Collins R (2008) SLCO1B1 variants and statin-induced myopathy--a genomewide study. *N Engl J Med* **359:**789-799.

Morimoto K, Oishi T, Ueda S, Ueda M, Hosokawa M and Chiba K (2004) A novel variant allele of OATP-C (SLCO1B1) found in a Japanese patient with pravastatin-induced myopathy. *Drug Metab Pharmacokinet* **19:**453-455.

Niemi M, Pasanen MK and Neuvonen PJ (2011) Organic anion transporting polypeptide 1B1: a genetically polymorphic transporter of major importance for hepatic drug uptake. *Pharmacol Rev* **63:**157-181.

Peng SX, Rockafellow BA, Skedzielewski TM, Huebert ND and Hageman W (2009) Improved pharmacokinetic and bioavailability support of drug discovery using serial blood sampling in mice. *J Pharm Sci* **98:**1877-1884.

Pfaffl MW (2001) A new mathematical model for relative quantification in real-time RT-PCR. *Nucleic Acids Res* **29:**e45.

Prasad B, Evers R, Gupta A, Hop CE, Salphati L, Shukla S, Ambudkar S and Unadkat JD (2013) Interindividual Variability in Hepatic Oatps and P-Glycoprotein (ABCB1) Protein Expression: Quantification by LC-MS/MS and Influence of Genotype, Age and Sex. *Drug Metab Dispos*.

Prueksaritanont T, Chu X, Evers R, Klopfer SO, Caro L, Kothare PA, Dempsey C, Rasmussen S, Houle R, Chan G, Cai X, Valesky R, Fraser IP and Stoch SA (2014) Pitavastatin is a more sensitive and selective OATP1B clinical probe than rosuvastatin. *Br J Clin Pharmacol*.

Shitara Y, Maeda K, Ikejiri K, Yoshida K, Horie T and Sugiyama Y (2013) Clinical significance of organic anion transporting polypeptides (OATPs) in drug disposition: their roles in hepatic clearance and intestinal absorption. *Biopharm Drug Dispos* **34:**45-78.

Takane H, Kawamoto K, Sasaki T, Moriki K, Kitano H, Higuchi S, Otsubo K and Ieiri I (2009) Life-threatening toxicities in a patient with UGT1A1*6/*28 and

SLCO1B1*15/*15 genotypes after irinotecan-based chemotherapy. *Cancer Chemother Pharmacol* **63:**1165-1169.

U.S. Department of Health and Human Services FaDA, Center for Drug Evaluation and Research (CDER). (2012.) Guidance for industry, drug interaction studies—study design, data analysis, implications for dosing, and labeling recommendations. . *http://www.fda.gov/downloads/Drugs/GuidanceComplianceRegulatoryInformation/Guidances/ucm292362.pdf*.

van de Steeg E, Stranecky V, Hartmannova H, Noskova L, Hrebicek M, Wagenaar E, van Esch A, de Waart DR, Oude Elferink RP, Kenworthy KE, Sticova E, al-Edreesi M, Knisely AS, Kmoch S, Jirsa M and Schinkel AH (2012) Complete OATP1B1 and OATP1B3 deficiency causes human Rotor syndrome by interrupting conjugated bilirubin reuptake into the liver. *J Clin Invest* **122:**519-528.

van de Steeg E, van Esch A, Wagenaar E, Kenworthy KE and Schinkel AH (2013) Influence of Human OATP1B1, OATP1B3, and OATP1A2 on the Pharmacokinetics of Methotrexate and Paclitaxel in Humanized Transgenic Mice. *Clin Cancer Res* **19:**821-832.

van de Steeg E, Wagenaar E, van der Kruijssen CM, Burggraaff JE, de Waart DR, Elferink RP, Kenworthy KE and Schinkel AH (2010) Organic anion transporting polypeptide 1a/1b-knockout mice provide insights into hepatic handling of bilirubin, bile acids, and drugs. *J Clin Invest* **120:**2942-2952.

Williamson B, Soars AC, Owen A, White P, Riley RJ and Soars MG (2013) Dissecting the relative contribution of OATP1B1-mediated uptake of xenobiotics into human hepatocytes using siRNA. *Xenobiotica* **43:**920-931.

Yoshida K, Maeda K and Sugiyama Y (2012) Transporter-mediated drug--drug interactions involving OATP substrates: predictions based on in vitro inhibition studies. *Clin Pharmacol Ther* **91:**1053-1064.

Zimmerman EI, Hu S, Roberts JL, Gibson AA, Orwick SJ, Li L, Sparreboom A and Baker SD (2013) Contribution of OATP1B1 and OATP1B3 to the disposition of sorafenib and sorafenib-glucuronide. *Clin Cancer Res* **19:**1458-1466.

Footnotes

LS and XC contributed equally to this paper.

Financial support:

Nico Scheer and Anja Rode are employees of TaconicArtemis GmbH, a subsidiary of Taconic Farms Inc, who market the mice described in the manuscript.

Reprint requests:

Nico Scheer, PhD, TaconicArtemis, Neurather Ring 1, 51063 Koeln, Germany.

Tel.: +49 221 9645343; Fax: +49 221 9645321; Email: nico.scheer@taconicartemis.com

Figure Legends

Fig. 1. Liver gene expression in WT, Oatp1a/1b KO, hOATP1B1, and hOATP1B3 mice. (A) Expression of selected Slc and Abc transporters, and (B) metabolic enzymes in WT (black columns), Oatp1a/1b KO (red columns), hOATP1B1 (blue columns), and hOATP1B3 (green columns) was determined by TaqMan RT-PCR. Expression of each target gene is relative to the average Gapdh and β-Actin expression level within a given sample. The dashed line represents the limit of quantitation. All values represent the mean ± SD of n=3 mice/genotype.

Fig. 2. OATP1B1 and OATP1B3 protein expression in liver tissues from human and hOATP1B1 and hOATP1B3 mice. Measurements of OATP1B1 and OATP1B3 protein levels in human livers (black columns) were described previously (Prasad et al., 2013). Expression of the human transporters in livers from hOATP1B1 (blue column) and hOATP1B3 (green column) mice, respectively, were determined from n=5 mice from each line as described in the Materials and Methods. Values shown are mean ± SD.

Fig. 3. Uptake time profile of $E_2$17βG, CCK-8, TEA, and TCA in hepatocytes isolated from Oatp1a/1b KO, hOATP1B1, hOATP1B3, and WT mouse livers and the inhibition of uptake by several inhibitors. Time-dependent uptake of $E_2$17βG (0.1 μM) (A), CCK-8 (0.01 μM) (C), TEA (0.1 μM) (E), and TCA (0.1 μM) (G) was determined in hepatocytes isolated from Oatp1a/1b KO (red circles), hOATP1B1 (blue circles), hOATP1B3 (green circles), and WT (black circles) mouse livers at 37^{o}C. *, $P < 0.01$, statistically significant compared with Oatp1a/1b KO mice. Inhibitory effect of RIF SV (100 μM), rifampin (200 μM), CsA (10 μM), quinidine (100 μM), and BSP (100 μM) on uptake (measured at 3 min at

DMD Fast Forward. Published on May 22, 2014 as DOI: 10.1124/dmd.114.057976
This article has not been copyedited and formatted. The final version may differ from this version.

37°C) of $E_2$17βG (0.1 μM) (B), CCK-8 (0.01 μM) (D), TEA (0.1 μM) (F), and TCA (0.1 μM) (H) were also measured. *, P < 0.01, statistically significant compared with corresponding no inhibitor controls. Values shown are mean ± SD for experiments performed in triplicate.

Fig. 4. Uptake time profile of pitavastatin, rosuvastatin, pravastatin, and atorvastatin in hepatocytes isolated from Oatp1a/1b KO, hOATP1B1, hOATP1B3, and WT mouse livers and the inhibition of uptake rate by several inhibitors. Time-dependent uptake of pitavastatin (0.1 μM) (A), rosuvastatin (0.01 μM) (C), pravastatin (0.1 μM) (E), and atorvastatin (0.1 μM) (G) were determined in hepatocytes isolated from Oatp1a/1b KO (red circles), hOATP1B1 (blue circles), hOATP1B3 (green circles), and WT (black circles) mouse livers at 37°C. *, P < 0.01, statistically significant compared with Oatp1a/1b KO mice. Inhibitory effect of RIF SV (100 μM), rifampin (200 μM), and CsA (10 μM) on uptake rate (measured at 3 min at 37°C) of pitavastatin (0.1 μM) (B), rosuvastatin (0.01 μM) (D), pravastatin (0.1 μM) (F), and atorvastatin (0.1 μM) (H) were also measured. *, P < 0.01, statistically significant compared with corresponding no inhibitor controls. Values shown are mean ± SD for experiments performed in triplicate.

Fig. 5. Pravastatin blood concentration-time profiles and liver to blood concentration ratio in WT, Oatp1a/1b KO, hOATP1B1, hOATP1B3 and hOATP1B1/1B3 mice. Pharmacokinetic profile after 5 mg/kg IV (A, D) or PO (B, E) administration of pravastatin to male WT (black circles), Oatp1a/1b KO (red circles), hOATP1B1 (blue circles) and hOATP1B3 mice (green circles) (A, B) in a first study and male WT, Oatp1a/1b KO and hOATP1B1/1B3 (orange circles) mice (D, E) in a second study. Values shown are mean ± SD of n=4 mice per strain for both studies. Liver-to-blood concentration ratio (C) after IV and PO administrations of 5 mg/kg pravastatin in WT (black columns), Oatp1a/1b KO (red columns),

hOATP1B1(blue columns) and, hOATP1B3 (green columns) and FVB WT mice (black columns). Values shown are mean ± SD of n=3 mice per strain. *, $P < 0.05$, statistically significant compared to Oatp1a/1b KO mice.

Fig. 6. Pitavastatin plasma concentration-time profiles and liver-to-plasma concentration ratio in WT, Oatp1a/1b KO, hOATP1B1, and hOATP1B3 mice. (A) Pharmacokinetic profiles after 5 mg/kg PO administration of pitavastatin to male WT (black squares), Oatp1a/1b KO (red squares), hOATP1B1 (blue squares) and hOATP1B3 (green squares) mice. (B) Liver-to-plasma concentration ratios at 0.25, 2 and 8 hours after 5 mg/kg PO administration of pitavastatin in male WT (black columns), Oatp1a/1b KO (red columns), hOATP1B1(blue columns), and hOATP1B3 (green columns) mice. Values shown are mean ± SD of at least three mice per strain. *, $P < 0.05$, statistically significant compared to Oatp1a/1b KO mice.

Fig. 7. Rosuvastatin blood concentration-time profiles in WT, Oatp1a/1b KO, hOATP1B1, and hOATP1B3 mice. Pharmacokinetic profiles after 5 mg/kg IV (A) or 15 mg/kg PO (B) administration of rosuvastatin to male WT (black squares), Oatp1a/1b KO (red squares), hOATP1B1 (blue squares) and hOATP1B3 (green squares) mice. Values shown are mean ± SD of n=4 mice per strain.

DMD Fast Forward. Published on May 22, 2014 as DOI: 10.1124/dmd.114.057976
This article has not been copyedited and formatted. The final version may differ from this version.

Tables

TABLE 1

PK parameters after IV and PO administrations of 5 mg/kg pravastatin to FVB WT, Oatp1a/1b KO, hOATP1B1, hOATP1B3 and hOATP1B1/1B3 mice (values reported as mean ± SD; n=4 mice). NC; not calculated.

	Mouse line	IV Administration		PO Administration	
		CL (ml/min/kg)	$AUC_{0\text{-}2hr}$ (μM*hr)	$AUC_{0\text{-}2hr}$ (μM*hr)	C_{max} (μM)
Study 1	FVB WT	150 ± 22[a]	1.32 ± 0.20[a]	0.045 ±0.01[a]	0.07 ± 0.04[a]
	Oatp1a/1b KO	36 ± 2.8	5.46 ± 0.40	0.81 ± 0.33	0.68 ± 0.35
	hOATP1B1	45 ± 9.1	4.50 ± 0.81	0.39 ± 0.06[a]	0.39 ± 0.14
	hOATP1B3	56 ± 7.4[a]	3.55 ± 0.48[a]	0.17 ± 0.06[a]	0.16 ± 0.05[a]
Study 2	FVB WT	132 ± 8.9[a]	1.49 ± 0.11[a]	NC	NC
	Oatp1a/1b KO	39 ± 3.6	5.07 ± 0.48	0.86 ± 0.22	0.74 ± 0.18
	hOATP1B1/1B3	83 ± 13[a]	2.39 ± 0.36[a]	0.23 ± 0.04[a]	0.22 ± 0.07[a]

[a] Significantly different from Oatp1a/1b KO mice ($p<0.05$).

DMD Fast Forward. Published on May 22, 2014 as DOI: 10.1124/dmd.114.057976
This article has not been copyedited and formatted. The final version may differ from this version.

TABLE 2

PK parameters after 5 mg/kg PO administration of pitavastatin to FVB WT (n=12), Oatp1a/1b KO, hOATP1B1, hOATP1B3 mice (n=9 for all three lines). PK calculations were performed as a group analysis due to the experimental design (see Materials and Methods).

Mouse line	**PO Administration**	
	$AUC_{0\text{-}8hr}$ (μM*hr)	C_{max} (μM)
FVB WT	0.33 ± 0.1	0.39 ± 0.17
Oatp1a/1b KO	3.87 ± 0.55	5.27 ± 2.64
hOATP1B1	3.70 ± 0.92	4.59 ± 1.12
hOATP1B3	4.01 ± 0.47	6.91 ± 0.63

DMD Fast Forward. Published on May 22, 2014 as DOI: 10.1124/dmd.114.057976
This article has not been copyedited and formatted. The final version may differ from this version.

TABLE 3

PK parameters after IV (5 mg/kg) and PO (15 mg/kg) administrations of rosuvastatin to FVB WT, Oatp1a/1b KO, hOATP1B1 and hOATP1B3 mice (values presented as mean ± SD; n=4)

Mouse line	IV Administration		PO Administration	
	CL (ml/min/kg)	$AUC_{0\text{-}24hr}$ (μM*hr)	$AUC_{0\text{-}24hr}$ (μM*hr)	C_{max} (μM)
FVB WT	88.8 ± 28.0[a]	2.45 ± 0.96[a]	0.08 ± 0.02[a]	0.04 ± 0.02[a]
Oatp1a/1b KO	31.2 ± 7.20	5.73 ± 1.58	3.80 ± 0.95	1.39 ± 0.50
hOATP1B1	29.5 ± 12.2	7.02 ± 2.33	4.09 ± 0.93	3.30 ± 1.77
hOATP1B3	28.5 ± 9.9	7.35 ± 3.41	3.14 ± 0.85	0.75 ± 0.12[a]

[a] Significantly different from Oatp1a/1b KO mice ($p<0.05$).

Figure 1

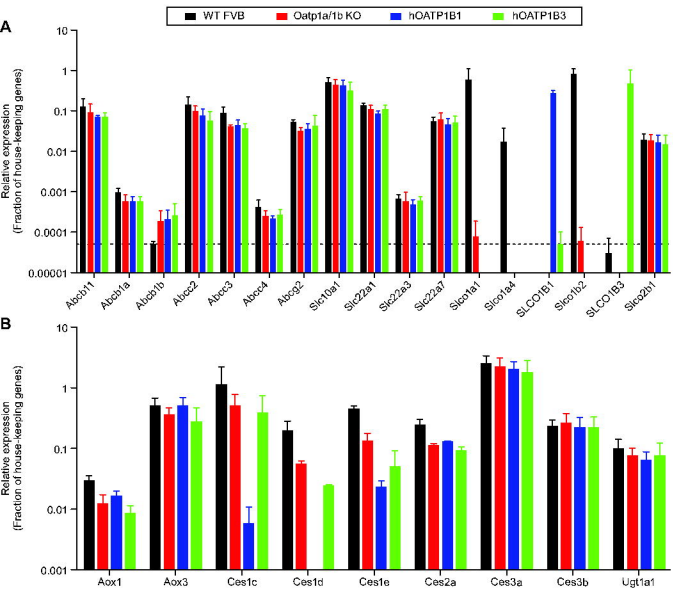
WT FVB
Oatp1a/1b KO
hOATP1B1
hOATP1B3
A
Relative expression
(Fraction of house-keeping genes)
10
1
0.1
0.01
0.001
0.0001
0.00001
Abcb11
Abcb1a
Abcb1b
Abcc2
Abcc3
Abcc4
Abcg2
Slc10a1
Slc22a1
Slc22a3
Slc22a7
Slco1a1
Slco1a4
SLCO1B1
Slco1b2
SLCO1B3
Slco2b1
B
Relative expression
(Fraction of house-keeping genes)
10
1
0.1
0.01
0.001
Aox1
Aox3
Ces1c
Ces1d
Ces1e
Ces2a
Ces3a
Ces3b
Ugt1a1

Figure 2

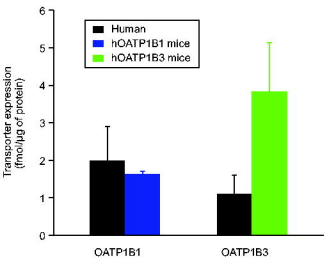
Human
hOATP1B1 mice
hOATP1B3 mice
Transporter expression
(fmol/µg of protein)
0
1
2
3
4
5
6
OATP1B1
OATP1B3

Figure 3

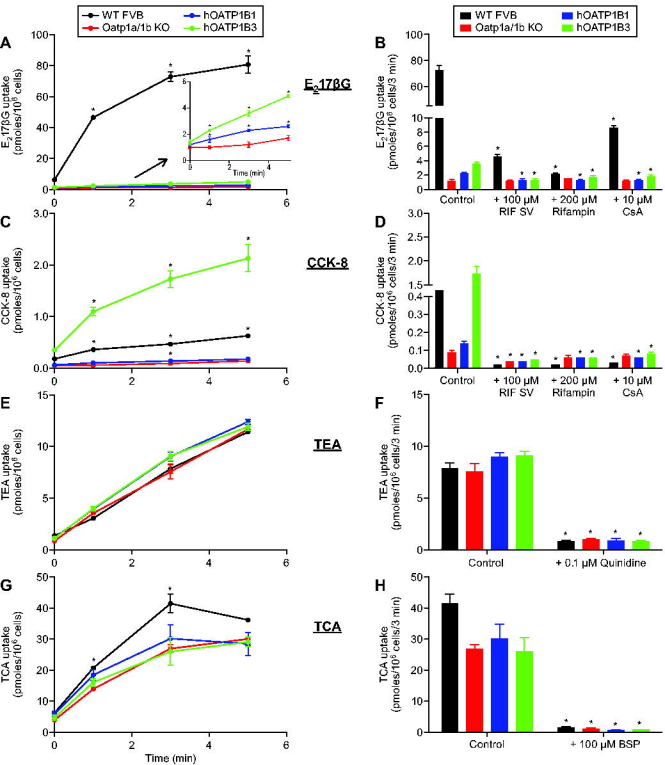
WT FVB
Oatp1a/1b KO
hOATP1B1
hOATP1B3
A
B
C
D
E
F
G
H
E2 17βG
CCK-8
TEA
TCA
E2 17βG uptake (pmoles/10^6 cells)
E2 17βG uptake (pmoles/10^6 cells/3 min)
CCK-8 uptake (pmoles/10^6 cells)
CCK-8 uptake (pmoles/10^6 cells/3 min)
TEA uptake (pmoles/10^6 cells)
TEA uptake (pmoles/10^6 cells/3 min)
TCA uptake (pmoles/10^6 cells)
TCA uptake (pmoles/10^6 cells/3 min)
Time (min)
Control
+ 100 µM RIF SV
+ 200 µM Rifampin
+ 10 µM CsA
+ 0.1 µM Quinidine
+ 100 µM BSP

Figure 4

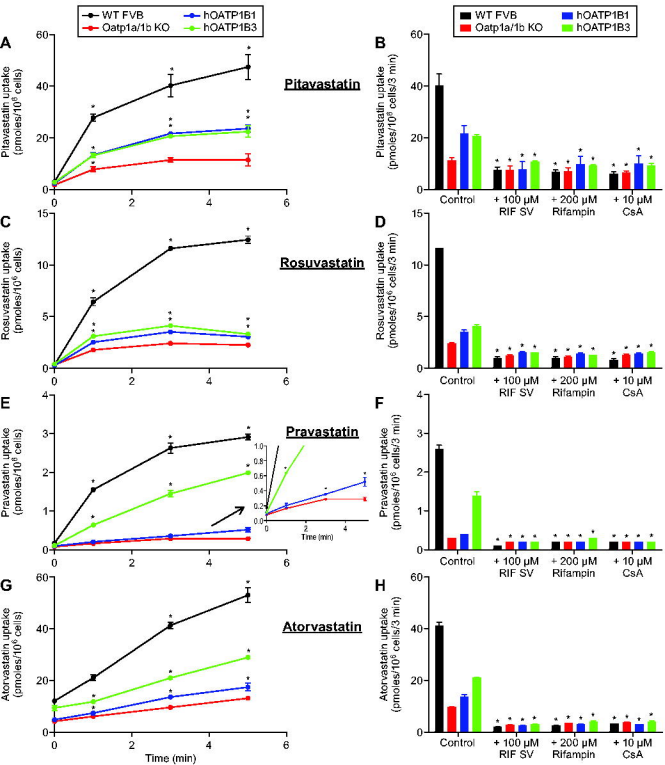
WT FVB
Oatp1a/1b KO
hOATP1B1
hOATP1B3
A
B
C
D
E
F
G
H
Pitavastatin
Rosuvastatin
Pravastatin
Atorvastatin
Pitavastatin uptake (pmoles/10^6 cells)
Rosuvastatin uptake (pmoles/10^6 cells)
Pravastatin uptake (pmoles/10^6 cells)
Atorvastatin uptake (pmoles/10^6 cells)
Pitavastatin uptake (pmoles/10^6 cells/3 min)
Rosuvastatin uptake (pmoles/10^6 cells/3 min)
Pravastatin uptake (pmoles/10^6 cells/3 min)
Atorvastatin uptake (pmoles/10^6 cells/3 min)
Time (min)
Control
+ 100 µM RIF SV
+ 200 µM Rifampin
+ 10 µM CsA

Figure 5

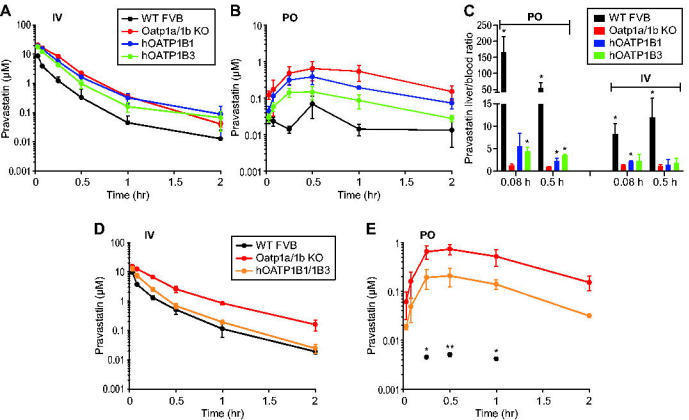
A
IV
WT FVB
Oatp1a/1b KO
hOATP1B1
hOATP1B3
Pravastatin (μM)
Time (hr)
B
PO
C
PO
IV
Pravastatin liver/blood ratio
0.08 h
0.5 h
D
IV
hOATP1B1/1B3
E
PO

Figure 6

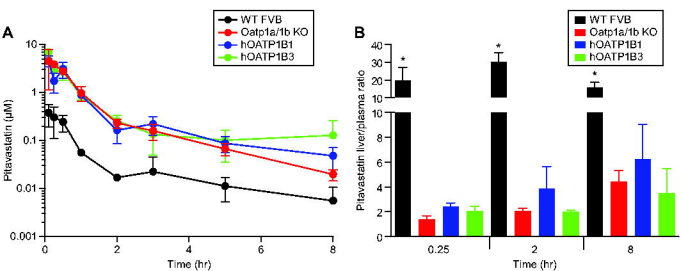
A
WT FVB
Oatp1a/1b KO
hOATP1B1
hOATP1B3
Pitavastatin (μM)
10
1
0.1
0.01
0.001
0
2
4
6
8
Time (hr)
B
WT FVB
Oatp1a/1b KO
hOATP1B1
hOATP1B3
Pitavastatin liver/plasma ratio
40
30
20
10
10
8
6
4
2
0
*
*
*
0.25
2
8
Time (hr)

Figure 7

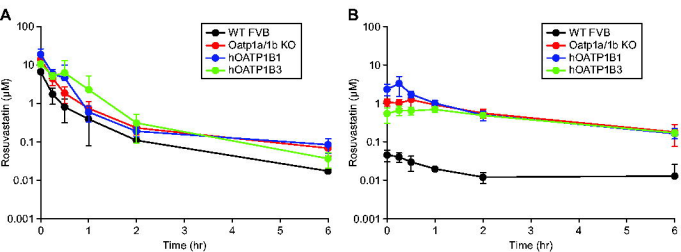
A
B
WT FVB
Oatp1a/1b KO
hOATP1B1
hOATP1B3
Rosuvastatin (μM)
Time (hr)
100
10
1
0.1
0.01
0.001
0
1
2
3
4
5
6